Structural Engineering and Mechanics, Vol. 6, No. 7 (1998) 827-839
DOI: http://dx.doi.org/10.12989/sem.1998.6.7.827

Buckling of the multi-vaulted "Aster" shell under axial compression alone or combined with an external pressure

M. Araar† and M. Derbali‡

University of Annaba, Institute of Civil Engineering, B.P 12, 23000 Annaba, Algeria

J.F. Jullien‡†

INSA of Lyon - 20 Av. Albert Einstein, 69621 Villeurbanne Cedex, France

Abstract. This paper presents a study of buckling of the multi-vaulted cylindrical shell ("Aster"), under an axial compression alone or combined with an external pressure. This shell which was presented in a recent paper is a self-stiffened structure having a satisfactory behaviour and a higher buckling strength under external pressure than a circular cylindrical shell with the same dimensions. The results of this study emphasize the interest of the behaviour of the "Aster" shell under two other types of loading, revealing an acceptable level of strength which is favorable for an expansion of its use in other areas.

Key words: buckling; cylindrical shell; "Aster" shell; axial compression; external pressure; combined loading; self stiffening.

1. Introduction

With the aim of contributing to the self stiffening of cylindrical shell vs buckling, an intensive research was carried out at the INSA of Lyon on quasi-perfect cylindrical shells, under external pressure. This study allowed us to elaborate a new shape of self-stiffened shell called "Aster". It is a multi-vaulted cylindrical shell with an optimal number of vaults, for which a patent was obtained (Jullien and Araar 1990). It shows a higher buckling strength under external pressure, in comparison with circular cylindrical shells having the same characteristics (Araar and Jullien 1996).

We have studied the possibility to extend the application of this shell to other areas where it would be subjected to axial compression or to a combination of this load with an external pressure (stanchions of offshore structures e.g.). For this purpose we worked out an experimental study on the behaviour of a such shell under these two modes of loading with reference to the circular cylindrical shell as comparison.

† Senior Lecturer
‡ Doct. Candidate
‡† Professor

This paper presents the results of this study after a brief review of the elaboration principle of the shape of this shell.

2. Review of the elaboration principle of the "Aster" shell

We remind that the geometry of the "Aster" shell has been elaborated after an intensive study on the behaviour of quasi-perfect circular cylindrical shells under external pressure. This study permitted to notice that precritical shape of theses shells is modal and that a mode close to the critical one is the governing one. This "pilot" mode is induced by geometrical imperfections of curvature oriented towards the inside of the shell and having a shape close to the critical mode. The number of waves of the precritical geometry is unavoidable, we decided to opposite the circumferential modal shape. This is obtained by creating a multiple vaults along the circumferential surface of the shell with straight meridian and curvatures oriented exclusively towards the outside. The optimal number of vaults of this shell is equal to twice the circumferential critical buckling mode of circular shell (Fig. 1). The depth of vaults is a parameter affecting the shell strength.

3. Methodology of the study

The experimental investigation of the shell "Aster" under axial compression alone or combined with an external pressure is conducted on specimens similar to those used for the case of the external pressure alone (Araar and Jullien 1996). These specimens have 22 vaults with 2.3 mm depth and a radius of 20 mm.

The comparison of results is done with two other type of shell:

- a circular cylindrical shell called "referential" and a shell with multiple vaults called V.M14. The later has 14 vaults of 2,35 mm depth and 35 mm as radius.

The dimensional characteristics of the three shells are given in Fig. 2 and their average values are given below:

L (mm)	R (mm)	h (Microns)	E (MPa)
120	75	140 to 150	(155 to 163) 10^3

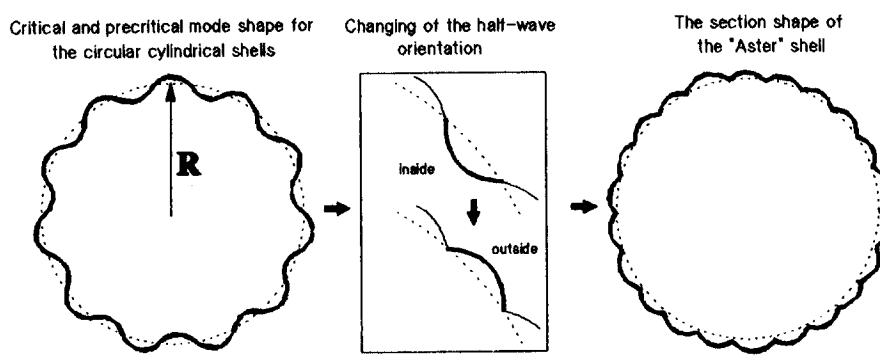

Fig. 1 The elaboration principle of the "Aster" shell

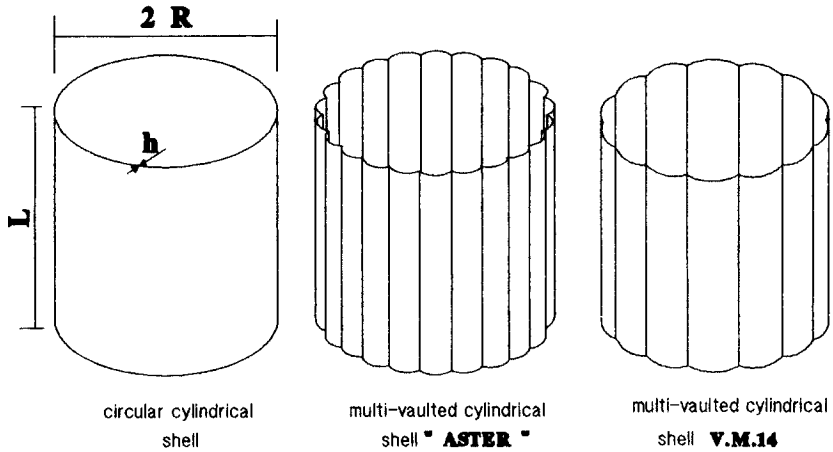

Fig. 2 Geometry of the studied shells

The different notations are at the end of the paper.

We bear in mind that different specimens were obtained by depositing Nickel electrolitically on patterns having the same geometry of the specimens and covered by a conductor layer of graphite. The loading in compression is applied by imposed displacement in the case of compression alone, and by an imposed force in the case of combined loading. The pressure is obtained by depression inside the specimens.

The end supports of the specimens were close to the fixed type.

4. Behaviour under axial compression

4.1. The geometry changes under loading

In the case of referential circular cylindrical shells, from the first load increments the precritical geometry takes a modal shape in both direction, axial and circumferential, and increases with the increase of loading. From the data obtained in both directions, it is noticed that the mode which occured along the shell is nearly the same as the one at the critical stage. This means that the critical level will be governed essentially by the state of imperfections in that direction.

The results obtained by Waeckel (1984), for similar cylindrical shells consider only initial imperfections mesured along parallels. As the overall modal imperfection is the one most affects the critical load, the author showed that an imperfection of this type having a value of 50% of the thickness off the shell could reduce the critical load by 50% of that of an ideal shell with the same dimensions. That means that the initial geometrical imperfections observed on the referential shell will have a predominant effect on the expected critical loads.

Concerning the multi-vaulted shells "Aster" and VM14, their geometry progressed outwards axisymetrically, according to a zero mode in the circumferential direction and a part-sine-wave outwards for the axial direction. This mode seems at first to be more favorable than that of the referential shells especially toward the geometrical initial imperfections effect.

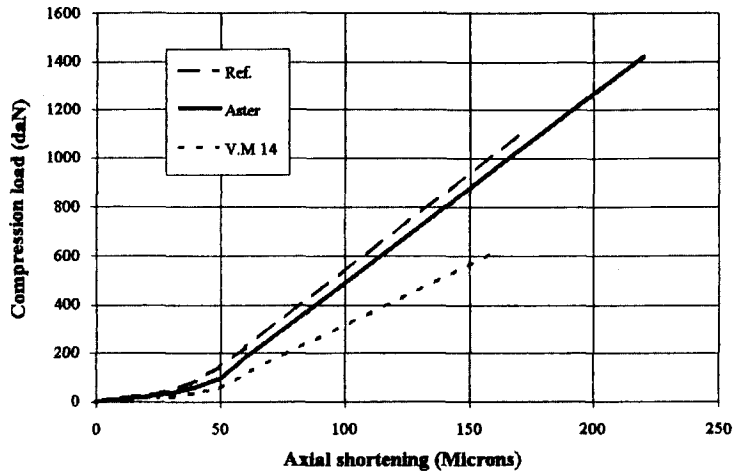

Fig. 3 Behaviour of the different shells

Table 1 Critical compression loads for different shells

Shell	h (Mic.)	E (MPa)	F_{exp} (daN)	F_{cl} (daN)	F_{exp}/F_{cl}	F_{exp}/F_{ref}
Referential	150	163000	1100	1395	0.79	–
Aster	153	162000	1420	1440	0.99	1.29
V.M.14	148	156500	620	1304	0.48	0.56

4.2. Critical states

The three tested type of shells have a linear elastic behaviour up to the instability state by bifurcation (Fig. 3). The non-linear part at the beginning of all curves is associated to the adjustment of specimens in the testing device.

The bifurcation is obtained for the mean loads given in Table 1, with other parameters to make easier the comparison of the results.

The classical critical load F_{cl} is given by the formula (Timoshenko 1966):

$$F_{cl} = \frac{2\pi E h^2}{\sqrt{3(1-\nu^2)}}$$

This load is computed for referential circular cylindrical shells tested experimentaly. It is also computed for shells of the same type and having identical characteristics of multi-vaulted shells of comparison.

In the Table 1, F_{ref} is the experimental critical load of compression of referential shells, for which a mean value of 1100 daN is used for comparison with the other shells.

For the referential shells the difference of 21% of the experimental critical load compared to the theoritical load F_{cl} is principally related to geometrical imperfections as it is mentioned above.

The experimental critical load of the "Aster" shell is about 30% greater than that of the referential one. If we accept a comparable state of imperfection between the two shells, the

last difference shows a better resistance of the "Aster" shell.

As it is shown in Table 1, the VM14 shell has a lower critical load (a difference of more than 50%) compared to the referential and the "Aster" shells. This corroborates the previous constatation and justify the optimal character of the number of vaults of the "Aster" shell.

4.3. Post-critical state

Fig. 4 gives the shape of the post-critical geometry of the referential shells (developed as a Fourier's series), indicating the existence of several modes between 10 and 14. This geometry is established with the same amplitudes in both directions, axial and circumferential, and is generalized in a cylindrical portion of the shell.

The post-critical geometry of the "Aster" shell is characterised by the formation of hollow

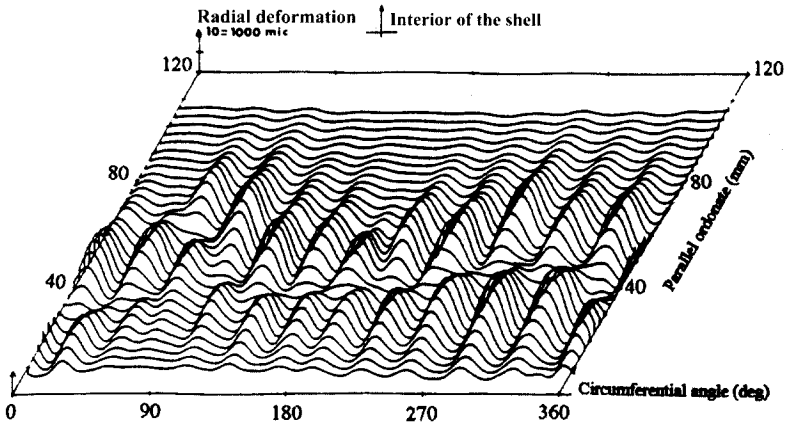

Fig. 4 Post-critical geometry developped in Fourier's series for the circular cylindrical shells under axial compression

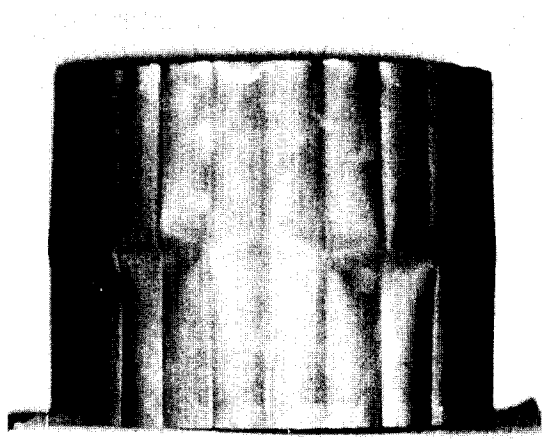

Fig. 5 Post-critical state of the "Aster" shell under axial compression

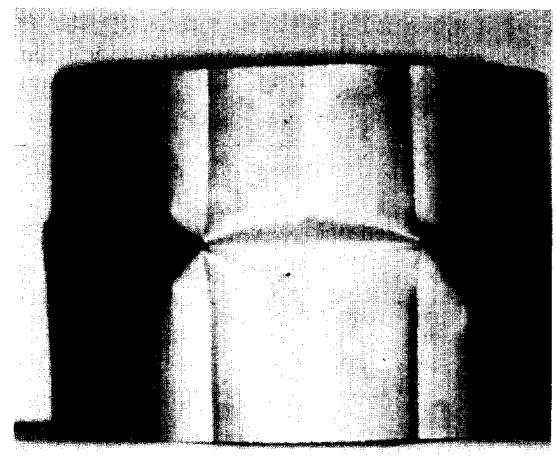

Fig. 6 Post-critical state of the V.M.14 shell under axial compression

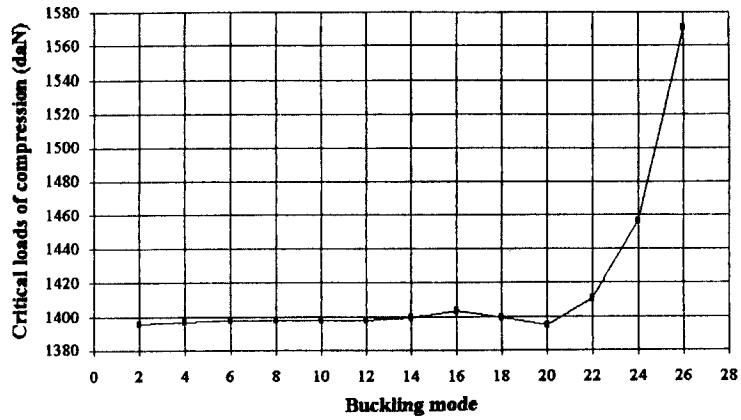

Fig. 7 The spread of the critical state on several modes.

waves with maximum to the right of singularities according to mode 11 (Fig. 5). The amplitude of these waves is lower than that of the deformed referential shell.

The buckled shape of shell V.M.14 (Fig. 6) is homothetic to that of the "Aster" shell, this let us to believe that the multi-vaulted shells have a comparable critical mode in axial compression. This is not the case for referential shells. The local curved areas which are formed at the junction of vaults and at mid-height of the shell have an amplitude greater for the case of the shell V.M.14. They disappear when the load is removed, this could be due to a lower stiffness of the V.M.14 shells, and therefore justify the decrease of their critical load.

4.4. Numerical computing

The evaluation of the critical load for circular cylindrical shells using a finite element code presents no difficulties and gives results in agreement with the theory. The spread of the critical geometry on many modes observed experimentally is corroborated by numerical computing, which indicates a minimum of energy on many harmonics as shown in Fig. 7.

For the multi-vaulted shells, it is necessary to use sophisticated models. A carefull discretisation of such shells is required to compute their critical loads and modes. These exigences lead us to bring out a simplified method for designing the "Aster" shell under such loading. This will be the subject of another paper with a similar approach for the external pressure case.

5. The behaviour under combined loading

The results showed that in the case of independent loading, external pressure and axial compression, the radial axisymetrical displacements are in opposite direction respectively. This lead us to study the behaviour of the "Aster" shell under the combination of such loadings with the aim of finding it better than that of the circular cylindrical shells. The circular cylindrical shells behaviour was firstly analysed under the same type of loading. This was done to master the parameters affecting that behaviour and producing data for the purpose of comparison.

The V.M.14 shells were not studied for this type of loading because of their lower strength under the external pressure alone (Araar and Jullien 1996), or under the axial compression alone as it was mentioned.

5.1. Behaviour of circular cylindrical shells

Many buckling tests were done on circular cylindrical shells for many values of pressure and compression couples. Moreover for the comparison with the "Aster" shell, these experimental and numerical results allowed us to compare with other author's prediction, theories and design rules.

Both pressure and compression are applied in a coupled manner with a constant ratio K between the membrane circumferential stress σ_θ (PR/h) and axial stres σ_x ($F/2\pi Rh$), this ratio is written as: $K=F/2\pi R^2P$.

The ratios between the critical loads P_c and F_c under combined loading, and the critical loads under loadings applied independently, are computed with considering for the latter the values F_1 and P_1 obtained from numerical competing using INCA CODE of system CASTEM of CEA (France). These two loads are determined for each specimen taking into account its geometrical and mechanical properties and assuming that both ends are clamped. This procedure is envisaged to allow plotting the interaction curves on the same graphe and to take into account geometrical and mechanical differences of all tested specimens.

The ratios used for the presentation of different interaction curves are:

$$R_x = F_c/F_1 \qquad R_p = P_c/P_1$$

The following table gather the different experimental results as well those for the case of compression alone ($K=\infty$) and pressure alone ($K=0$).

The computed results using the INCA CODE for different values of K are summarized in

Table 2 Critcal loads for circular cylindrical shells under combined loading

Specimen	h Micr.	E MPa	K	P_c mbars	P_1 mbars	R_p	F_c daN	F_1 daN	R_x
1	150	162800	0	210	246	0.86	0	0	0
2	142	155000	4	164	213	0.77	218	1280	0.17
3	145	163000	8	160	226	0.71	450	1345	0.33
4	148	155000	16	120	227	0.53	670	1335	0.5
5	139	155900	26	75	198	0.38	680	1200	0.57
6	137	160000	50	45	194	0.23	780	1180	0.66
7	150	163000	∞	0	0	0	1100	1440	0.76

Table 3 Numerical results of the INCA Code

K	∞	39	28	17	7	3	0
F_{cr}	1440	1382	1213	936	503	220	0
P_{cr}	0	100	124	159	201	227	246
R_x	1	0.96	0.84	0.65	0.35	0.153	0
R_p	0	0.41	0.51	0.65	0.82	0.92	1

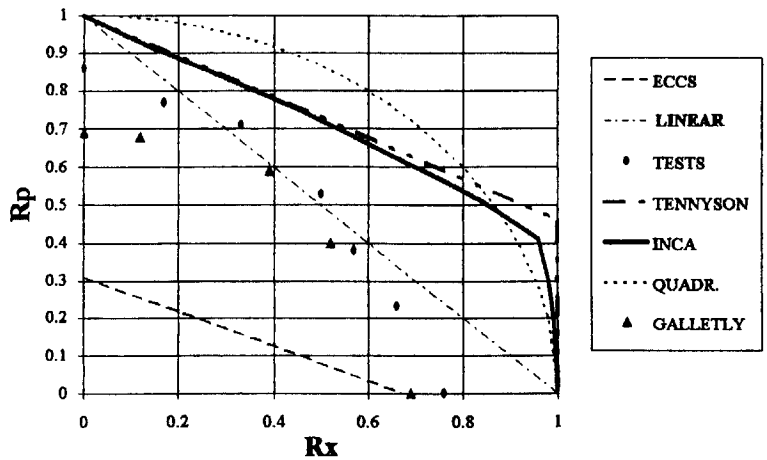

Fig. 8 Interaction curves

Table 3.

The different interaction curves are given in Fig. 8 in which we can see:

(1) the experimental curve
(2) the numerical curve INCA
(3) the linear interaction ($R_x+P_p=1$)
(4) the ECCS prediction curve (ECCS 1983)
(5) the quadratic interaction ($R_x^2+R_p^2=1$)
(6) Tennyson's curve (Tennyson, Booton and Chan 1978)
(7) Galletly's curve (Galletly, James, Kruzlecki and Pemsing 1987).

From this figure we can comment on three groupes of similar curves. The first group gathers Tennyson's curve, the quadratic interaction and the INCA curve. The latter is enveloped by the two others.

The second group gathers the experimental, the linear and the Gallety's curves. The experimental points are systematically below the curves of the first group, with a difference increasing when the compression becomes significant.

The last group is the linear interaction of the ECCS rules, which is conservative and more so when the external pressure is predominant.

The homothety between the experimental and the INCA curves is relatively fullfilled when the external pressure is predominant. This is justified by the geometrical imperfections effect under such sollicitation.

Gallety's curve is below the experimental curve because of the low value of Bathtorf's parameter Z ($Z\approx 50$) of the specimens studied by this author as well as because of the welding effect. These two effects cumulate the influence of geometrical imperfections, boundary conditions and the residual stresses.

Concerning the behaviour of the tested shells, and with a target of comparison with the "Aster" shell, particular attention is given for the interaction of different circumferential modes. We insist on the evolution of the radial displacements at different points of the shell, in paticular at points where the curvature is inwards.

When applying both loadings, a movement of modal precritical waves is observed, either by a modal change or by their displacement over the shell surface (Fig. 9).

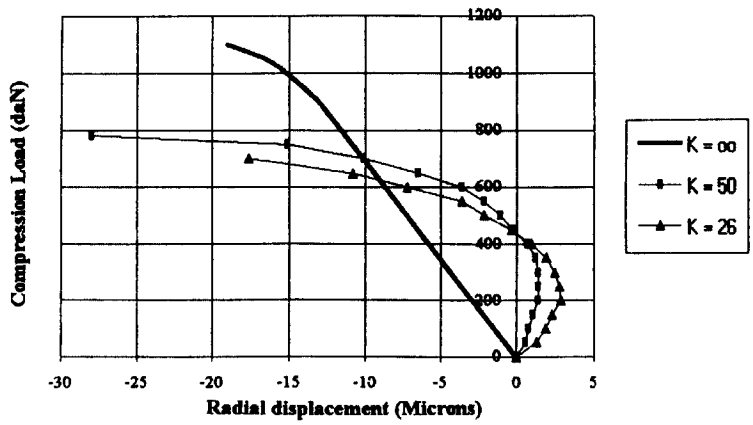

Fig. 9 Evolution of the radial displacement at mid-high of the referential shell (in the hollow defect)

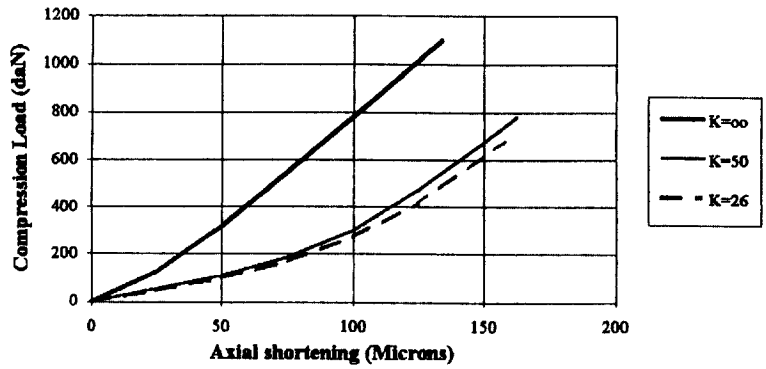

Fig. 10 Evolution of the axial shortening for several values of K

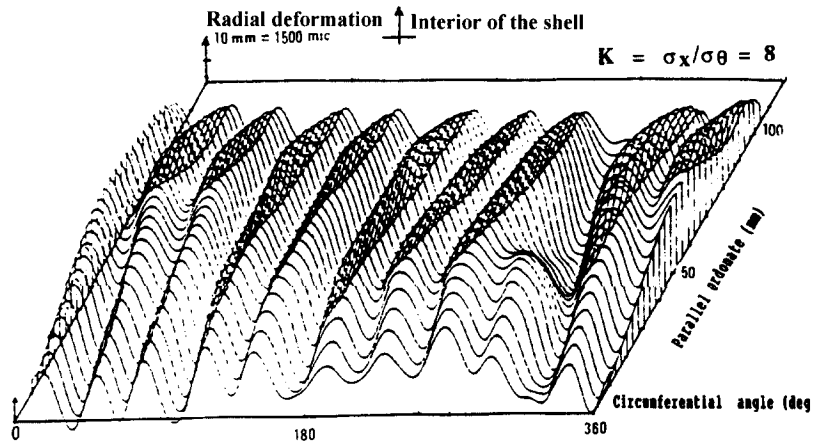

Fig. 11 Post-critical geometry developped in Fourier's series for the circular cylindrical shells under combined loading

Comparatively to the behaviour of the shell under axial compression alone, the superposition of both solicitations conducts to a decrease of the initial axial stiffness of the

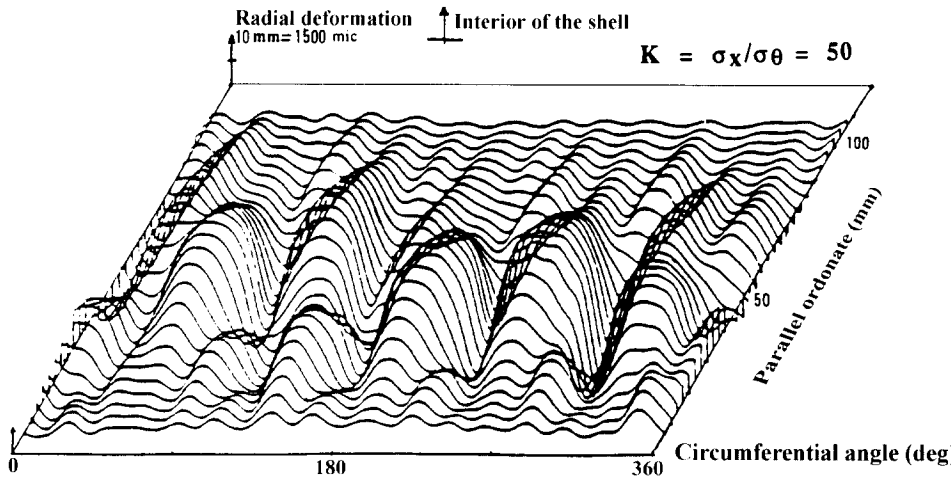

Fig. 12 Post-critical geometry developed in Fourier's series for the circular cylindrical shells under combined loading

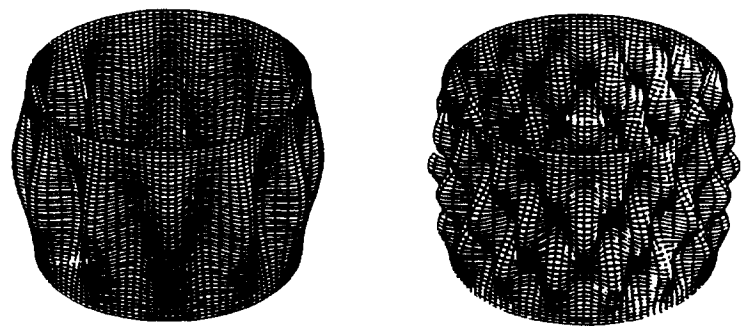

Fig. 13 Calculated post-critical geometry of the circular cylindrical shell under combined loading

shell (Fig. 10). The non-linearities due to the setting of specimens into the testing device are reduced when an axial load of about 250 daN is applied.

The precritical and post-critical modes have a shape governed by the dominant solicitation (Figs. 11, 12).

The numerical computing shows also the modal interaction mentioned above (Fig. 13). It shows that the instability mode is governed essentially by the external pressure.

The effect of the compression is seen to occur for high values of R_x ($R_x > 0$, 9), characterized by the brutal change in the shape of the INCA curve.

5.2. Behaviour of "Aster" shells

Four specimens were tested with differents ratios of combined loads. The results are given in Table 4, where it is given for the cases of uniaxial compression and external pressure, applied separately.

Table 4 Critical loads for the "Aster" specimens under combined loading

Spécimen	h Micr.	E MPa	K'	P_c mbars	P_1 mbars	R_p	F_c daN	F_1 daN	R_x
1	155	161000	0	920	245	3.74	0	1440	0
2	142	160000	0.7	543	194	2.80	250	1177	0.21
3	140	148000	1.4	380	167	2.28	450	1025	0.44
4	140	160000	1.8	326	194	1.68	790	1177	0.67
5	152	163000	3.5	205	246	0.833	1484	1440	1.03
6	153	162000	∞	0	246	0	1420	1440	0.99

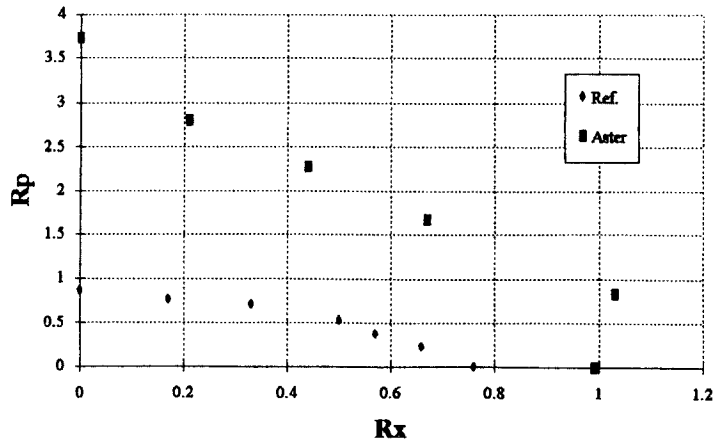

Fig. 14 Comparaison of the interaction curves of the referential and "Aster" shells

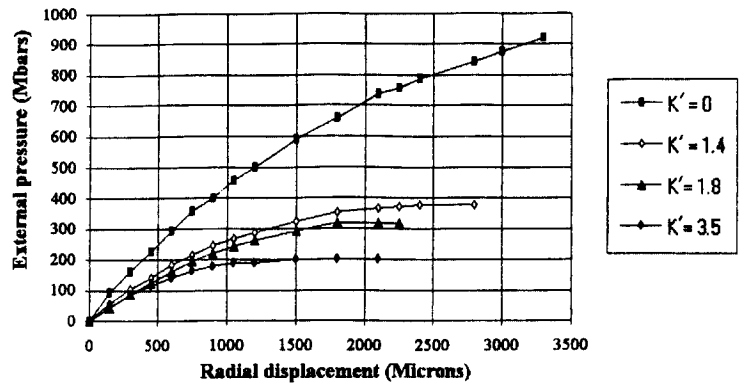

Fig. 15 Evolution of the radial displacement in the vault summit at mid-high of the "Aster" shell

Since it is difficult to express the circumferential stresses for such geometry, to determine the loading parameter $K=\sigma_x/\sigma_\theta$ by analogy to referential shells, we consider another parameter K' defined as it follows.

Let P_o be the critical pressure for the "Aster" shell under external pressure alone and F_o is its critical compression under uniaxial compression alone. The critical pressure and compression under combined loading are respectively P_c and F_c, with $P_c=\beta P_o$. The loading

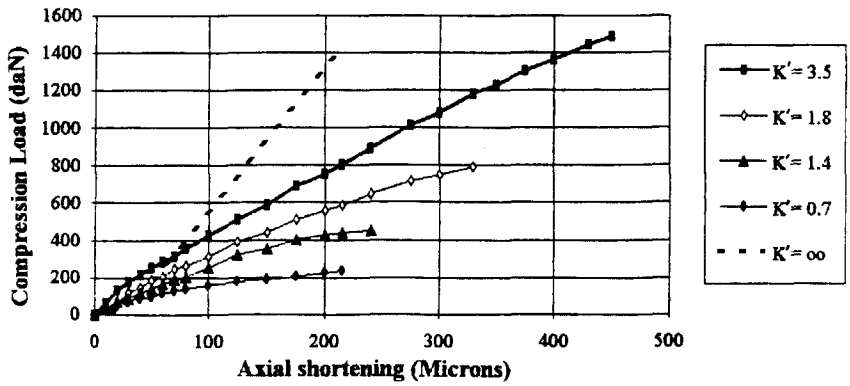

Fig. 16 Evolution of the axial shortening of the "Aster" shell for several values of K'

path is choosen by considering a linear interaction $P/P_o+F_c/F_o=1$. The parameter K' is defined as $K'=(F/F_o)/(P/P_o)=(1-\beta)/\beta$. Both loading are applied so that the ratio F/P remains constant and equal to $(F_o/P_o)*K'$.

To allow for comparison with the referential shells, we have computed for each tested specimen the ratios R_p and R_x, on the basis of the critical loads under external pressure alone (P_1) and compression alone (F_1). Both loads are computed for the circular cylindrical shell with identical characteristics to the "Aster" shell.

The results in Table 4, presented in the interaction diagram of Fig. 14, express the advantage allows by the "Aster" shell compared to the circular cylindrical shell.

Concerning the evolution of the geometry of the shell, the lateral displacements remains axisymetric. We can notice the effect of the pressure eventhough small, characterized by a considered radial displacement (Fig. 15). This displacement is accompanied by a shortening of the shell combined to that produced by the axial compression (Fig. 16). The axial stiffness is varying with the ratio of both loads and decreases with the increase of the external pressure rate.

6. Conclusions

The experimental results presented in this paper lead to a better strength of the "Aster" shell in axial compression compared to circular cylindrical shells with the same characteristics. They also showed the optimal aspect of the number of vaults under this solicitation.

When the axial compression is combined with an external pressure, the shell still has better strength, especially when one of the two solicitations is predominant.

References

Araar, M., Jullien, J.F. (1996), "Buckling of cylindrical shells under external pressure-proposition of a new shape of self-stiffened shell", *Int. J. of Structural Engineering and Mechanics*, **4**(4), 451-460.

ECCS (1981, 1983), "European convention for constructional steel work section 4.6", (buckling of shells, the construction press, London, 1981), (also ECCS Pub. n° 29, Brussels, 1983).

Galletly, G.D., James, S., Kruzlecki, J. and Pemsing, K. (1987), "Interactive buckling tests on cylinders subjected to external pressure and axial compression", *Journal of Pressure Vessel Technology*, **109**, 10-18.

Jullien, J.F. and Araar, M. (1990), "Coque à haute résistance à géomérie de révolution", Brevet n° 90. 04277, Lyon - France, 23 mars 1990.

Tennyson, R.C., Booton, M. and Chan, K.H. (1978), "Buckling of short cylinders under combined loading", *Trans. ASME*, **45**, 574-578.

Timoshenko, S. (1966), "Théorie de la stabilité élastique", Ed. DUNOD, Paris.

Waeckel, N. (1984), "Stabilité des plaques et des coques - influence des défauts géométriques initiaux", Thése de Doctorat d'Etat, INSA de Lyon - France.

Notations

R	Interior radius of diffent shells
r	Vault's radius
L	Lengt betwen support of different specimens
h	Thikness
E	Young's modulus
ν	Poisson's coefficient
P	External pressure
F	Axial compression
P_1	Critical load under external pressure alone, calculated with the INCA code for the referential cylindrical shells
F_1	Critical load under axial compression alone, calculated with the INCA code for the referential cylindrical shells
P_c	Critical pressure under combined loading
F_c	Critcal axial compression under combined loading
σ_θ	Membrane circumferential stress
σ_x	Membrane axial stress
K, K'	Loading parameters
R_p	P_c and P_1 ratio
R_x	F_c and F_1 ratio